molecular pharmaceutics

ARTICLE

pubs.acs.org/molecularpharmaceutics

Tumor Specific Delivery and Therapy by Double-Targeted Nanostructured Lipid Carriers with Anti-VEGFR-2 Antibody

Donghua Liu, Fengxi Liu, Zhihong Liu, Lili Wang, and Na Zhang*

School of Pharmaceutical Sciences, Shandong University, 44 Wenhua Xi Road, Ji'nan 250012, China

ABSTRACT: Vascular endothelial growth factor receptors (VEGFRs) are overexpressed on the surface of a variety of tumor cells and on tumor neovasculature in situ, which are potential targets for "double targeting" (tumor- and vascular-targeting) tumor therapy. This study aimed to develop a VEGFR-mediated drug delivery system to target chemotherapeutic agents to VEGFR-overexpressed tumor cells and tumor neovasculature endothelial cells *in vitro* and *in vivo*. An antibody modified docetaxel (DTX)-loaded targeted nanostructured lipid carrier (tNLC) was designed and prepared with DSPE-PEG-NH_2 as linker. The cellular cytotoxicity, cellular uptake, *in vivo* therapeutic effect and biodistribution of tNLC were investigated. The tNLC showed a particle size about 168 nm with encapsulation efficiency >95%, drug loading 5.55 ± 0.06% (w/w) and an average ligand coupling efficiency of 3.34 ± 2.63%. Cytotoxicity of tNLC against three human cell lines and one murine malignant melanoma was superior to that of Duopafei and nontargeted NLC (nNLC). The tNLC also showed better tolerance and antitumor efficacy in a murine model bearing B16 compared with Duopafei or nNLC. The studies on cellular uptake and biodistribution indicated that the better antitumor efficacy of tNLC was attributed to the increased accumulation of drug in both tumor and tumor vasculature. These findings suggested that tNLC designed to bind specifically to VEGFR-2 can be used to deliver DTX to the tumor vasculature and tumor and may inhibit tumor growth.

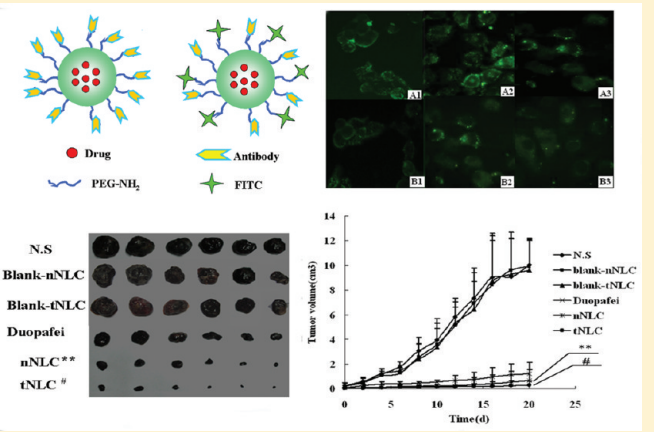

KEYWORDS: chemotherapy, docetaxel, double target, cytotoxicity, murine malignant melanoma, nanostructured lipid carriers

1. INTRODUCTION

Currently, chemotherapy still is the one of the most effective approaches to cancer treatment. However, the crucial problem in cancer chemotherapy is the adverse toxic side effects of anticancer drugs on healthy tissues.[1−4] In cancer therapy, more than 90% of therapeutic drugs is taken up by normal tissues, whereas only 2−5% is taken up by tumors.[1,4] Invariably the side effects impose dose reduction, frequent treatment or discontinuance of therapy. To improve the therapeutic efficacy and limit the severe side effects of cancer chemotherapy on healthy organs, research has focused on combinational treatment.[1]

Recently employed strategies of combinational treatment for cancer therapy are as follows. (1) Combination of two kinds of drugs. Combination of chemotherapeutic agents and angiogenesis inhibitor is now commonly employed in the clinic to treat cancer.[5] (2) Combination of two targeting ligands in one delivery system for "double targeting" tumor therapy.[6] The preparation of one delivery system with two targeting ligands is complicated, so the research about this strategy is minor.[6] Hence, the ideal strategy of active target chemotherapy would be a one targeting ligand medium drug delivery system that is targeted to both tumor cells and tumor neovasculature endothelial cells. The advantages of this one ligand for double targeting ("one-double targeting") strategy are obvious and include not only achieving the combinational treatment but also simplifying the manufacturing, while the crucial step of the one-double targeting strategy is to determine the one-double targeting ligand.

Vascular endothelial growth factors (VEGFs) are small polypeptide growth factors and appear to play important roles in angiogenesis and tumor growth.[7,8] VEGF receptors (VEGFRs) have been found to be overexpressed, in comparison to normal tissues, in breast, melanoma, carcinoma cervicis, gastric, and non-small-cell lung cancer[7] and on tumor neovasculature in situ.[8] Compared with VEGFs, VEGFRs are the better target for its overexpression on the surface of cell membrane.

Recently, the antibody of VEGFR is increasingly recognized as an efficient target ligand for cancer therapy, for targeting VEGFR-expressing tumor neovasculature.[9−11]

DC101 (the monoclonal rat anti-VEGFR-2 antibody) immunoliposomes (DC101-IL) displayed a 7-fold better binding to VEGFR-2-positive 293T cells (pFlk1-transfected immortalized human kidney cells) in comparison to unspecific liposomes.

Received: April 5, 2011
Accepted: September 16, 2011
Published: September 17, 2011

ACS Publications © 2011 American Chemical Society

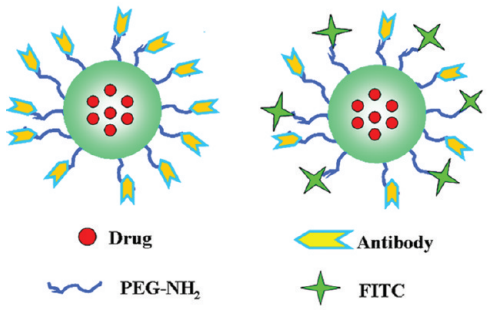

Figure 1. Schematic representation of the antibody-labeled and antibody, FITC-colabeled nanostructured lipid carriers.

Compared to blank DC101-IL, free doxorubicin and HEPES/glucose, the doxorubicin loaded DC101-IL led to a significant delay in tumor growth by delivering doxorubicin to the tumor endothelium.[9] Another study showed that the angiogenesiss and the growth of human glioblastoma cells in immunodeficient mice were inhibited by systemic treatment with a monoclonal antibody against VEGFR-2.[12] The results of a phase I study on weekly administration of IMC-1121B (human anti-VEGFR-2 antibody) showed that IMC-l121B can recognize VEGFR-2 and inhibit angiogenesis and tumor growth.[13] VEGFRs have been found to be also overexpressed in many cancer cells, and they would be connected with inducing proliferation and migration of cancer cells.[14] VEGFRs are overexpressed not only on tumor neovasculature but also in many cancer cells, which would directly target drug to tumor cells and neovasculature and inhibit tumor growth. Therefore, "one-double targeting" tumor therapies (tumor and vascular targeting) using anti-VEGFR-2 antibody would be implemented via a one drug delivery system based on the VEGFRs which have been verified to be overexpressed on both tumor neovasculature and cancer cells.

In this study, a one-double targeting drug delivery system prepared with DSPE-PEG-NH_2 as linker was developed, in which nanostructured lipid carriers (NLC) were used as drug carrier and anti-VEGFR-2 antibody as targeting ligand to deliver docetaxel (DTX) specifically to tumor and tumor neovasculatures which overexpress VEGFR-2 (Figure 1). The NLC are developed from a solid lipid nanoparticle (SLN) system.[15,16] The NLC system shares advantages of SLN, e.g. controlled drug release, biocompatibility and the possibility of production on a large industrial scale. DTX is a mitotic spindle poison that accelerates the microtubule assembly from tubulin and blocks the depolymerization of the microtubule.[17] It has demonstrated extraordinary anticancer effects both *in vitro* and *in vivo* against a variety of tumors including lung, ovaries, breast, leukemia, malignant melanoma, etc.[16,18,19] Flk-1(A-3) is a mouse monoclonal anti-VEGFR-2 antibody raised against amino acids 1158−1345 mapping at the C-terminus of the VEGFR-2 (Flk-1). Flk-1(A-3) could recognize VEGFR-2 of mouse, rat and human origin.

Considering the important role of the angiogenic vessels in tumor growth, the cytotoxicity and cellular uptake of nontargeted NLC (nNLC) and Flk-1(A-3) modified NLC (tNLC) were investigated against VEGFR-2 overexpressed human umbilical vein endothelial cells (HUVEC). HUVEC has for many years been the canonical endothelial cell model system.[20] Murine malignant melanoma (B16) overexpresses VEGFR-2 specifically, and the level of expression of VEGFR-2 is high in microvasculature of subcutaneously inoculated B16 tumor.[21,22] So, *in vivo* antitumor efficacy and the biodistribution studies were carried out in Kunming mice bearing B16. Here we report for the first time that "one-double targeting" tumor therapies (tumor- and vascular-targeting) using Flk (A-3) would be implemented via a one drug delivery system, and antitumor efficacy of this system against malignant melanoma was evaluated.

The aim of this study is to evaluate the one-double targeting strategy on tumor target chemotherapy. The *in vitro* cytotoxicity of Duopafei, nNLC and tNLC against two human cancer cell lines, B16 and HUVEC, were evaluated. The cellular uptake, *in vivo* therapeutic effect and biodistribution of tNLC comparing nNLC and Duopafei were investigated.

2. MATERIALS AND METHODS

2.1. Materials. Injectable soya lecithin (phosphatidylcholine accounts for 95%, pH = 5.0−7.0) was provided by Shanghai Taiwei Pharmaceutical Co., Ltd. (Shanghai, China). Pluronic F68 (F68) was provided by Aladdin Co., Ltd. (Shanghai, China). Stearic acid, glyceryl monostearate and middle chain triglycerides were purchased from Shanghai Chineway Pharm. Tech. Co., Ltd. (Shanghai, China). Duopafei was provided by Qilu Pharmaceutical Co., Ltd. (Jinan, China). 1,2-Distearoyl-*sn*-glycero-3-phosphoethanolamine-*N*-[amino(polyethylene glycol)-2000] (DSPE-PEG-NH_2) was purchased by Avanti Polar Lipids Inc. (Alabaster, AL, USA). Anti-VEGFR-2 antibody (Flk-1(A-3)) was purchased by Santa Cruz Biotechnology Inc. (USA). Biotin and *N*-hydroxylsuccinimide were purchased from Aladdin Reagent Database Inc. (Shanghai, China). Avidin-FITC was provided by Wuhan Boster Bioengineering Limited Co. (Wuhan, China). The homobifunctional cross-linker bis[sulfosuccinimidyl] suberate (BS3) was purchased by Sigma Chemical Inc. (St. Louis, MO, USA). All the other chemicals and reagents used were of analytical purity grade or higher, obtained commercially.

Human hepatocellular liver carcinoma (HepG2), lung adenocarcinoma (A549), murine malignant melanoma (B16) and human normal hepatocellular (HL-7702) cells were obtained from Shandong Institute of Immunopharmacology and Immunotherapy (Shandong, China). Human umbilical vein endothelial cells (HUVEC) were purchased from ScienCell (Carlsbad, CA, USA).

2.2. Synthesis of Biotin-*N*-hydroxysuccinimide. Biotin-NHS was prepared from biotin and *N*-hydroxysuccinimide (NHS) by coupling with dicyclohexylcarbodiimide (DCC). Briefly, dimethylformamide (DMF) was vacuum distilled in the presence of CaH_2. Biotin was dissolved into hot DMF, and then NHS and DCC were added (biotin:NHS:DCC = 1:1.2:1.2). The mixture was incubated at 50 °C for 16 h. The mixture was cooled to room temperature, and the dicyclohexylurea was filtered off. The filtrate was dried by the rotary evaporator. The residue was crystallized from isopropanol. The residue was refluxed in isopropanol and then filtered.

2.3. Synthesis of DSPE-PEG-biotin. DSPE-PEG (0.2 mmol) was added into DMF. After addition of NHS-biotin (1 mmol), the reactants were stirred overnight under nitrogen. The product was precipitated by the slow addition of diethyl ether, which was then filtered on a Buchner funnel and washed with diethyl ether. The molecular weight (MW) of product was confirmed by a time-of-flight mass spectrometer (TOF MS). Figure 2 shows the synthesis of DSPE-PEG-biotin.

2.4. Preparation of Nontargeted NLC (nNLC). The drug-loaded NLC were prepared by solvent diffusion method. Briefly, the desired amounts of stearic acid, glyceryl monostearate,

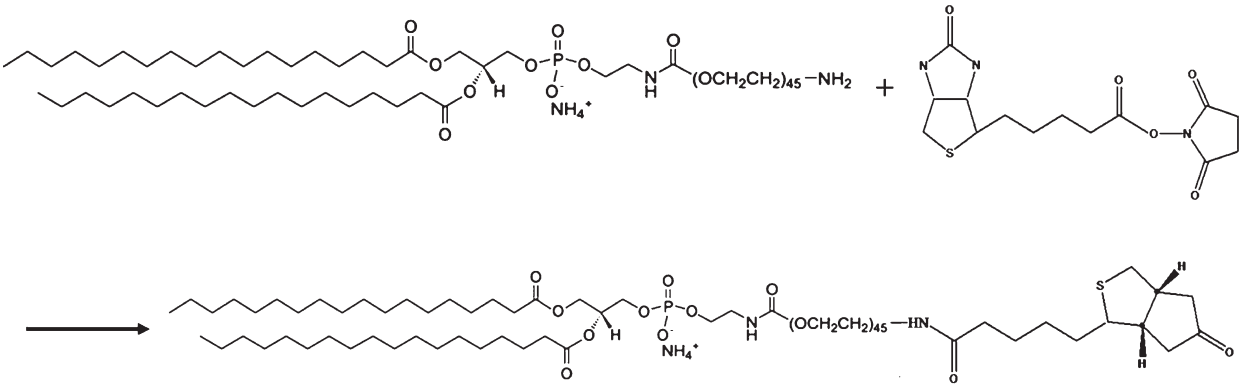

Figure 2. Scheme depicting the synthesis of DSPE-PEG-biotin.

soya lecithin, middle chain triglycerides, DSPE-PEG-NH_2 and DTX were dissolved in 1 mL of ethanol in a water bath at 70 °C. The organic phase was slowly (12 mL/h) injected by a microsyringe pump (KD Scientific, Holliston, MA, USA) into 10 mL of 1% F68 (w/v) aqueous solution, under mechanical agitation (DC-40, Hangzhou Electrical Engineering Instruments, China) with 500 rpm in a water bath at 70 °C for 10 min. Then DTX loaded PEG-NLC was obtained by solidification in an ice bath.

2.5. Preparation of Targeted NLC (tNLC). Using the procedure of Curnis et al.,[23] with slight modifications, the homobifunctional cross-linker bis[sulfosuccinimidyl] suberate (BS3) was used for the activation of DSPE-PEG(2000)-NH_2 in nNLC, which were then coupled to the amino group of the antibody of VEGFR-2. Briefly, nNLC were incubated for 30 min at room temperature with BS3 at a final concentration of 3 mM, and then purified, from unreacted cross-linker, by 0.5 mL of 3K Millipore (Amicon Ultra). "Activated NLC" were then collected, and antibody was added. After 2 h incubation at room temperature with gentle stirring, glycine was added at room temperature for 15 min at a final concentration of 50 mM in order to neutralize the unreacted lipidic groups. The antibody−NLC conjugates (tNLC) were then separated from free antibody by Millipore 0.5 mL (3K). The amount of free antibody was determined by the coomassie brilliant blue G-250 method. The ligand coupling efficiency was calculated by the formula $(W_{total} - W_{free})/W_{total}$.

2.6. Preparation of FITC-NLC. DSPE-PEG-biotin was added as lipids, and the NLC were prepared as above. Fluorescein isothiocyanate (FITC) was coupled with NLC through the biotin−avidin system. The avidin-FITC was dropped in NLC solution and then incubated for 1 h, and the avidin-FITC could be coupled with the biotin of the surface of NLC.

2.7. Determination of Entrapment Efficiency and Drug Loading. The desired amounts of nNLC and tNLC were dispersed in 2.9 mL of 0.5 wt % Tween 80−phosphate buffer solution (PBS, pH 7.4) and shaken (XW-80A, Instruments factory of Shanghai Medical University, China) for 3 min to dissolve the free drugs. The resulting dispersions were centrifuged for 10 min at 25,000 rpm (3K30, Sigma, Osterode am Harz, Germany). The drug content in the supernatant after centrifugation was measured by an HPLC method using an SPD-10Avp Shimadzu pump and an LC-10Avp Shimadzu UV−vis detector. Samples were determined by an HPLC method with the following conditions: Venusil XBP C-18 (4.6 mm × 250 mm, pore size 5 μm, Agela); mobile phase, acetonitrile:water (55:45, v/v); flow rate, 1.0 mL/min; and measured wavelength, 230 nm. The original NLC (0.01 mL) was dissolved in 0.49 mL of methanol, and the drug content in the original NLC was detected by the same HPLC method described above. The calibration curve of peak area against concentration of DTX was $A = 12684C - 722.76$ ($R = 0.9998$) under the concentration of DTX 1−50 μg/mL ($R = 0.9998$, where A = peak area and C = DTX concentration); the limit of detection was 0.02 μg/mL. The drug entrapment efficiency (EE) and drug loading (DL) of NLC were calculated from eqs 1 and 2:

$$EE\% = \frac{W_{total} - W_{free}}{W_{total}} \times 100 \quad (1)$$

$$DL\% = \frac{W_{total} - W_{free}}{W_{lipids}} \times 100 \quad (2)$$

W_{total}, W_{free} and W_{lipids} were the weight of drug added in system, analyzed weight of drug in supernatant and weight of lipid added to system, respectively

2.8. Characterization of NLC. The morphology of nNLC and tNLC was examined by transmission electron microscopy (JEM-1200EX, Japan). Samples were prepared by placing a drop of NLC suspension onto a copper grid and air-dried, following negative staining with a drop of 2% aqueous solution of sodium phosphotungstate for contrast enhancement.

The average diameter and polydispersity index were determined by laser light scattering (Zetasizer 3000SH, Malvern Instruments Ltd., Malvern, Worcestershire, England). Zeta potential was measured by laser Doppler anemometry (LDA) on a ZetaPlus zeta potential analyzer (Brookhaven Instruments Corporation, Holtsville, NY, USA). All measurements were performed at 25 °C. Calculation of the size and polydispersity indices was achieved using the software provided by the manufacturer. The diameter mean value was calculated from the measurements performed at least in triplicate.

2.9. *In Vitro* Release of DTX-Loaded Nanostructured Lipid Carriers. *In vitro* release of DTX from Duopafei, nNLC and tNLC was evaluated using a dialysis bag diffusion technique. Typically, 0.25 mL of DTX solution (2 mg/mL, Duopafei diluted with deionized water), 0.25 mL of nNLC and 0.25 mL of tNLC (2 mg/mL) were placed into a preswelled dialysis bag with 8−12 kDa molecular weight cutoff. DTX solution should be used immediately after dilution due to its instability. The bag was incubated in 15 mL of release medium (0.5% of Tween 80 in PBS, pH 7.4) at 37 °C under horizontal shaking.[24] At predetermined

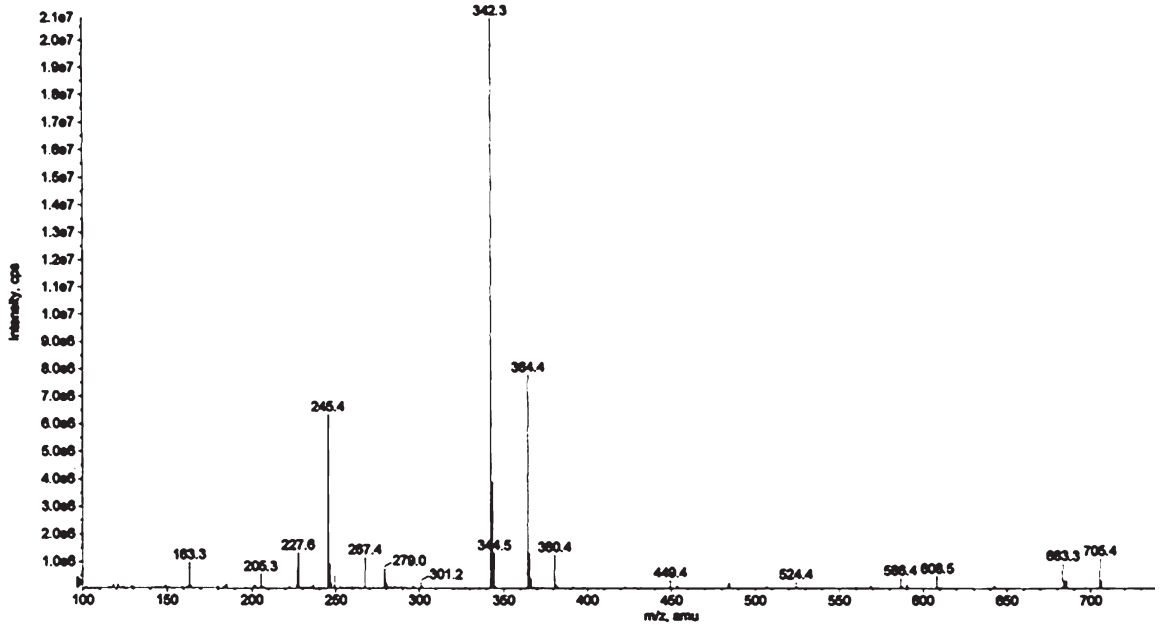

Figure 3. High resolution mass spectrum of the synthesized biotin-NHS.

time points, the dialysis bag was taken out and replaced into a new container filled with 15 mL of fresh medium.

The amount of DTX released was determined by an HPLC method with the following conditions: Venusil XBP C-18 (4.6 mm × 250 mm, pore size 5 μm, Agela); mobile phase, acetonitrile:water (1:1, v/v); flow rate, 1.0 mL/min; and measured wavelength, 230 nm.

2.10. *In Vitro* Cytotoxicity Studies. The cytotoxicity of Duopafei, nNLC and tNLC was tested in HepG2, A549 and mouse B16 cells using the MTT assay.[25] Briefly, cells were seeded in a 96-well plate at a density of 4000 cells/well and allowed to adhere for 24 h prior to the assay. Cells were exposed to a series of doses of Duopafei, nNLC and tNLC, respectively, at 37 °C. After 96 h of incubation, 20 μL of MTT (3-(4,5-dimethylthiazol-2-yl)-2,5-diphenyltetrazonium bromide) solution (5 mg/mL) was added to each well of the plate. After incubating for 4 h, 200 μL/well of DMSO was added to dissolve the contents in the plate, and the absorbance of the obtained DMSO solution was measured at 570 and 630 nm by a microplate reader (FL600, Bio-Tek Inc., Winooski, VT, USA). All experiments were repeated thrice.

2.11. Proliferation Inhibition on HUVEC. Proliferation inhibition of NLC was tested on human umbilical vein endothelial cells (HUVEC). HUVEC were seeded into 96-well plates and allowed to attach for 24 h. Cells were exposed to a series of doses of Duopafei, nNLC and tNLC, respectively, at 37 °C. Control group received culture medium only. After incubation for 96 h, 20 μL of MTT solution (5 mg/mL) was added to each well of the plate. After incubation for 4 h, 200 μL/well of DMSO was added, and the absorbance of the solution was measured at 570 nm and 630 nm by a microplate reader (FL600, Bio-Tek Inc.,Winooski, VT, USA). All experiments were repeated three times.

2.12. Fluorescence Microscopy and Flow Cytometry Analysis of NLC Incubated with B16, HUVEC and HL-7720 Cells. The internalization analysis of tNLC was characterized by incubation of B16, HUVEC and HL-7720 cells with FITC-labeled nNLC or tNLC. The B16, HUVEC and HL-7720 cells were seeded in a 12-well plate at a density of 2×10^5 cells per well and incubated overnight at 37 °C. At a confluence level of 70−80%, the growth medium was removed and the cells were washed twice with PBS buffer and replaced with serum medium or serum free medium. FITC-labeled nNLC or tNLC was added. The cells were then incubated for 1 h at 37 °C in the presence of either nNLC or tNLC at a concentration of 150 nM (2 mg/mL of total lipids) DTX. They were subsequently rinsed with PBS. GFP fluorescence in cells was observed using an inverted fluorescence microscope (λ_{ex}, 540 nm; λ_{em}, 580 nm; BX40, Olympus, Japan). After that, all cells were harvested for trypsinization and washed in PBS three times and cell-associated fluorescence was quantitatively determined by FACSCalibur flow cytometry (BD Biosciences, USA) by counting 10,000 events. Only the viable cells were gated for fluorescence analysis. All experiments were performed in triplicate.

2.13. *In Vivo* Antitumor Efficacy. The Kunming mice (female) used in this study were purchased from the Medical Animal Test Center of Shandong University, 6−8 weeks old and weighing about 15−18 g. All experiments were carried out in compliance with the requirements of the National Act on the use of experimental animals (People's Republic of China).

Mice implanted with B16 cell were used to qualify the efficacy of NLC administrated by intravenous injection. The mice were subcutaneously injected at the right axillary space with 0.1 mL of cell suspension containing 10^5 B16 cells.[26] Treatments were started after 8−10 days of implantation. The mice with tumor volume of ~50 mm^3 were selected, and this day was designated as day 0. The mice were randomly assigned to three treatment groups, with six mice in each group. Each group of mice was treated once a week by tail vein injection with the different formulations as described in the following: (A) physiological saline (N.S) as control group; (B) blank nNLC; (C) blank tNLC; (D) Duopafei (dosage of 20 mg/kg, diluted in physiological saline); (E) nNLC (dosage of 20 mg/kg); (F) tNLC (dosage of 20 mg/kg).

All mice were labeled, and tumors were measured every other day with calipers during the period of study. The tumor volume was calculated by the formula $(W^2 \times L)/2$, where W is the tumor

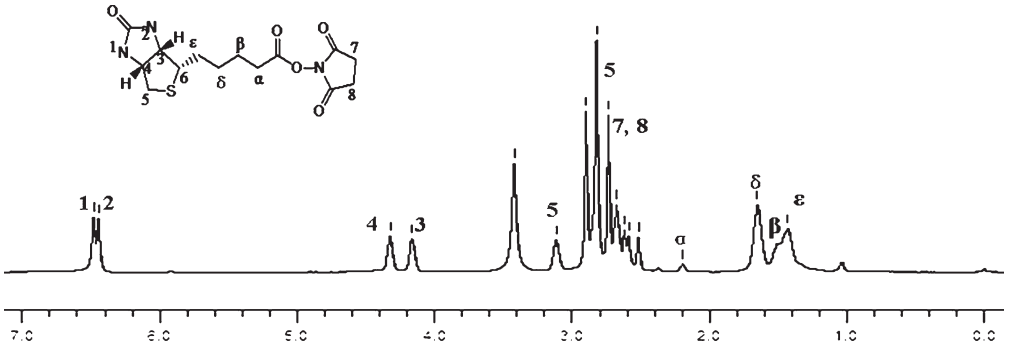

Figure 4. ^{1}H NMR spectra of the synthesized biotin-NHS in DMSO-d_6.

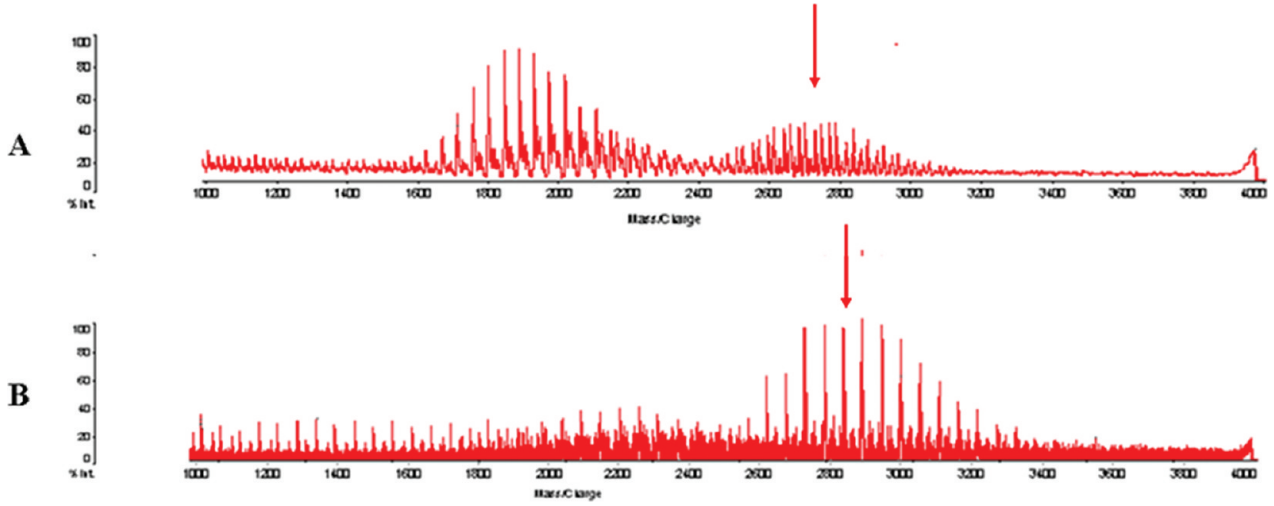

Figure 5. The time-of-flight mass spectra of DSPE-PEG-g-biotin: (A) DSPE-PEG-NH_2; (B) DSPE-PEG-g-biotin.

measurement at the widest point and L the tumor dimension at the longest point. Each animal was weighed at the time of treatment, so that dosages could be adjusted to achieve the mg/kg amounts reported. Animals also were weighed every other day during the experimental period. After 20 days, the tumors were dislodged and weighed.[27]

2.14. Pharmacokinetics and Tissue Distribution. Female Kunming mice bearing B16 (100−200 mm^3) were randomly assigned to three groups and injected intravenously through the tail vein with Duopafei (20 mg/kg), nNLC (20 mg/kg) or tNLC (20 mg/kg). In each group, blood samples which were taken from the retro-orbital plexus at predetermined time points (0.083, 0.25, 0.5, 0.75, 1, 2, 3, 4, 5, 6, 7and 8 h post iv dose) after drug administration (n = 5 at each time point) were centrifuged (4000 rpm, 15 min) and plasma was collected and stored. The mice were then sacrificed. The tumor, heart, liver, spleen, lung and kidney were collected, washed, weighed and homogenized (Ultraturrax homogenizer (IKS T10), IKAWerke GmbH & Co., Germany), and DTX was extracted with acetonitrile and methanol (v/v: 1:1). The amount of DTX in each tissue was determined by the HPLC assay as described above. The data were normalized to the tissue weight.

2.15. Pharmacokinetics and Statistical Analysis. The main pharmacokinetic parameters were calculated by the statistical moment method using the DAS 2.0 software. The area under the plasma concentration−time profiles (AUC), the distribution ($t_{1/2\alpha}$) and elimination half-life ($t_{1/2\beta}$), the mean residence time (MRT) and total plasma clearance (CL) were calculated. A two-tailed unpaired Student's t test was performed at $p < 0.05$.

3. RESULTS AND DISCUSSION

3.1. Synthesis of Biotin-NHS. The MW of biotin-NHS determined by high resolution mass spectrum (HRMS, Figure 3) was 342.3(100%, M^+, calculated 341.38 for $C_{14}H_{19}N_3O_5S$). The ^{1}H NMR spectrum of biotin-NHS (Figure 4) was measured in DMSO-d_6 using a 400 MHz spectrometer (Bruker Avance DPX 300): δ = 6.48 (1 H, NH-1), 6.44 (1H, NH-2), 4.16 (1H, NH-3), 4.32 (1H, NH-4), 3.11 (1H, NH-5A), 2.82 (1H, NH-5B), 2.75 (H-7,8), 2.19 (1H, H-α), 1.64 (H-β), 1.76 (H-δ), 1.43 (H-ε).

3.2. Synthesis of DSPE-PEG-g-biotin. Figure 5 showed time-of-flight mass spectra of DSPE-PEG-NH_2(A) and DSPE-PEG-g-biotin(B), which were determined by time-of-flight mass spectrometer. The average MW of DSPE-PEG-NH_2 was 2800-(Figure 5A), which was in accordance with the theoretical MW (2788.79). The experimental MW of DSPE-PEG-g-biotin determined by TOF MS being 3000 (Figure 5B) was in accordance with the theoretical MW (3014.68), which confirmed that the resulting synthetic product was the anticipant compound.

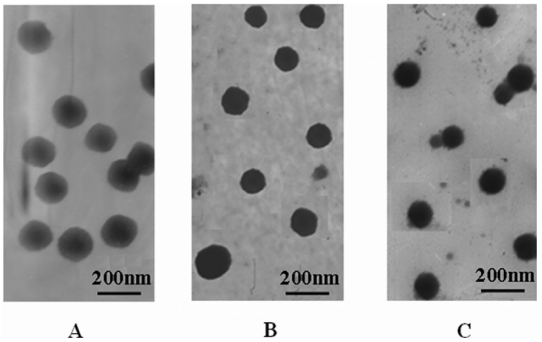

Figure 6. Transmission electron photomicrograms of NLC: (A) nNLC; (B) tNLC; (C) FITC-tNLC.

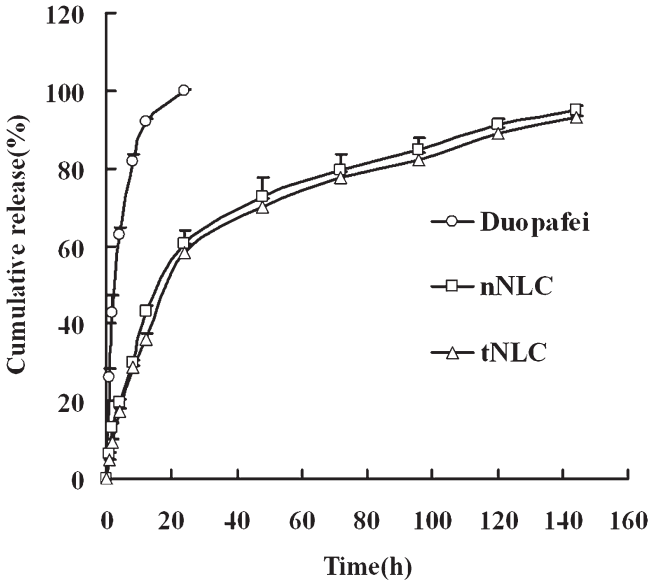

Figure 7. Release profiles of DTX-loaded NLC. Duopafei was used as free drug reference. Data were given as mean ± SD (n = 3).

3.3. Design, Preparation and Characterization of tNLC. For targeted drug delivery toward tumor, small molecule ligands, peptides, antibody and antibody fragments had all been used.[27,28] VEGFR is an important target for its overexpression in many cancers and on tumor neovasculature in situ. The targeting of therapeutics to tumor blood vessels, by probes that bind to specific molecular addresses on the vasculature, has become a major research area.[29] The inhibition of tumor growth via attack of the vascular supply of the tumor is now a validated target for anticancer therapy. In this study, a VEGFR-2 mediated drug delivery system (Figure 1) was developed, in which NLC was used as vector for drug delivery and anti-VEGFR-2 antibody as a targeting ligand to deliver DTX specifically to tumor cells and tumor neovasculatures (double targeting) which overexpress VEGFR-2.

The nNLC and tNLC were spherical or ellipsoidal in shape (Figure 6). The mean particle size of tNLC was 168.70 nm ± 2.07 nm (polydispersity index 0.195 ± 0.009) with zeta potential −28.89 ± 1.3 mV, entrapment efficiency 98.43 ± 0.51%, drug loading 5.55 ± 0.06% (w/w) and an average ligand coupling efficiency of 3.34 ± 2.63%. As control, nNLC showed the mean particle size 160.23 nm ± 2.57 nm (polydispersity index 0.212 ± 0.010), zeta potential −29.34 ± 1.73 mV, entrapment efficiency 93.24 ± 0.93% and drug loading 5.95 ± 0.07% (w/w). The mean size of FITC-tNLC was 162.23 ± 3.45 nm (polydispersity index 0.198 ± 0.010).

Table 1. IC50 of HepG2, A549 and B16 Cells Incubated with Duopafei, nNLC and tNLC at 96 h (n = 5)

cell line	Duopafei	nNLC	tNLC
HepG 2	0.96 ± 0.05	0.40 ± 0.06** [a]	0.27 ± 0.03[#]
A549	0.74 ± 0.02	0.12 ± 0.05**	0.06 ± 0.01[#]
B16	0.72 ± 0.10	0.35 ± 0.09**	0.21 ± 0.03[#]
HUVEC	1.96 ± 0.16	1.60 ± 0.07*	1.20 ± 0.06[##]

[a] $^{*}P < 0.05$, $^{**}P < 0.01$ versus Duopafei. $^{\#}P < 0.05$, $^{\#\#}P < 0.01$ versus nNLC.

3.4. *In Vitro* Drug Release. *In vitro* release profiles were obtained by representing the percentage of drug released with respect to the amount of DTX encapsulated in NLC (Figure 7). The release of DTX from tNLC followed the Weibull equation and could be expressed by the following equation: $\ln \ln(1/(1 - Q/100)) = 0.7669 \ln t - 2.8072$, $r = 0.9952$. DTX release profiles displayed a sustained release phase. This sustained release could mainly result from the erosion and degradation of the components of nanoparticles. The amount of cumulated drug released over 144 h was 93.1%. The release of DTX from nNLC followed the Weibull equation and could be expressed by the following equation: $\ln \ln(1/(1 - Q/100)) = 0.7199 \ln t - 2.5212$, $R = 0.9961$. The amount of cumulated drug released over 144 h was 95.2%. It was obvious that DTX released much more slowly from NLC than from Duopafei. In the first 24 h, only 50−60% DTX of NLC was released. In contrast, the release of DTX from Duopafei was fast and approximately 100% of the drug was released after incubation for 24 h.

3.5. *In Vitro* Cytotoxicity and Proliferation Inhibition on HUVEC. In order to know the activity of DTX-loaded NLC, *in vitro* cellular cytotoxicity was evaluated by MTT assay. The IC50 values of Duopafei, nNLC and tNLC for HepG2, A549 and B16 (n = 3) are presented in Table 1, respectively. Duopafei, nNLC and tNLC showed a clear dose-dependent cytotoxicity against these cells with DTX at an equivalent dose from 0.01 to 10 μM. tNLC has decreased the IC50 value for both cell lines, and there was statistical significance compared to nNLC, implying that tNLC show higher cytotoxicity against these cells. A possible mechanism underlying the enhanced efficacy of DTX against tumor cells may include the enhanced intracellular drug accumulation by ligand−receptor recognition.

There was statistical significance in the IC50 values of nNLC and Duopafei, implying that nNLC show higher cytotoxicity against these cells. The results are in accordance with previous studies that cytotoxicity of DTX-loaded nanoparticles was higher than that of free drugs.[30] A possible mechanism underlying the enhanced efficacy of DTX against B16 cells may include the enhanced intracellular drug accumulation by nanoparticle uptake.[31] On the other hand, blank nNLC and tNLC had no significant effects on the cell growth (data not shown). These negligible toxicity results observed for NLC, which are consistent with other reports,[32] could be explained by the low concentration of NLC present in the experimental conditions of the study.

The cytotoxicity of Duopafei, nNLC and tNLC was investigated against HUVEC. The IC50 values of Duopafei, nNLC and tNLC were calculated and are shown in Table 1, which presents

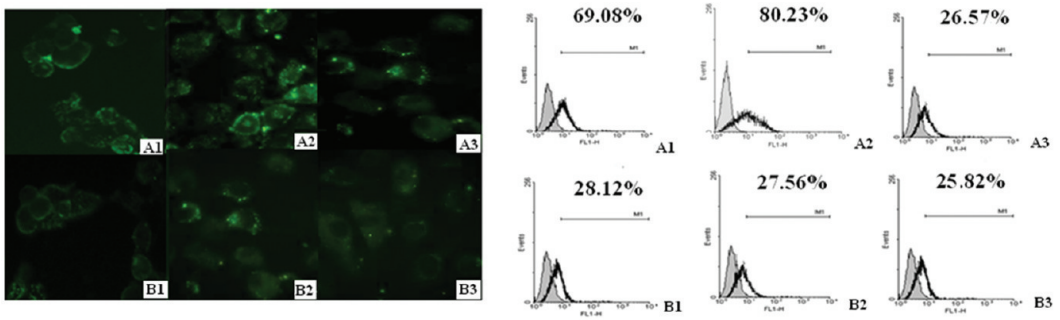

Figure 8. Fluorescence microscopy images and flow cytometry analysis of nNLC and tNLC ((A) tNLC; (B) nNLC; (1) B16 cells, (2) HUVEC cells, (3) HL-7702) in the presence of B16, HUVEC and HL-7702 cells after 1 h at 37 °C in the presence of 10% fetal bovine serum.

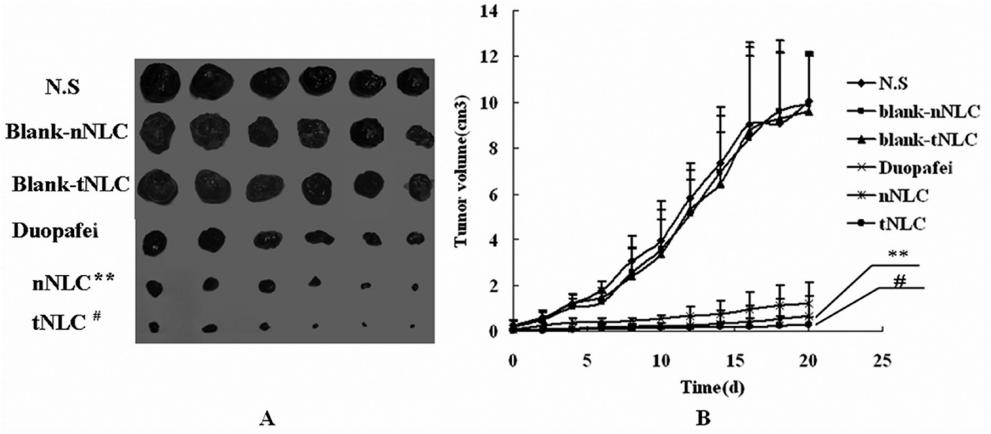

Figure 9. Antitumor effect of NLC. Data represent mean ± SD (n = 6). (A) Photographs of tumors from each treatment group excised on day 20. (B) Variation of tumor volume by intratumoral administration in B16 tumor-bearing mice. Note: $^{**}P < 0.01$ versus Duopafei. $^{\#}P < 0.05$ versus nNLC.

the *in vitro* inhibition of Duopafei, nNLC and tNLC for HUVEC (n = 3). There was statistical significance in the IC50 values of tNLC and nNLC, implying that tNLC had greater sensitivity to HUVEC compared to nNLC and could effectively inhibit the proliferation of tumor vessel endothelial cells. A possible mechanism would be in accordance with previous studies that the enhanced efficacy of DTX may include the enhanced intracellular drug accumulation by ligand−receptor recognition.

3.6. *In Vitro* Internalization of NLC. Functionalization of the NLC by the anti-VEGFR-2 antibody targeting ligand is first checked *in vitro*. FITC- labeled tNLC and nNLC are incubated in the presence of B16, HUVEC and HL-7702 cells. Figure 8 summarizes the results obtained both by fluorescence microscopy and flow cytometry after incubation with B16, HUVEC and HL-7702 cells. As shown in Figure 8, a little fluorescence was detected in cells incubated with nNLC after incubation with VEGFR-2-overexpressing B16 and HUVEC, whereas much higher fluorescence intensity was shown in cells treated with tNLC after 1 h incubation at 37 °C. Moreover, there were no differences in fluorescence intensity detected in cells treated with nNLC and tNLC after incubation with VEGFR-2-deficient HL-7702 cells. In the case of tNLC, internalization could be enhanced via the ligand−receptor recognition. It could be speculated that the higher cytotoxicity of tNLC compared with nNLC was mainly a result of better internalization. It could be speculated that tNLC designed to bind specifically to VEGFR-2 can be used to deliver DTX to the tumor vasculature and tumor cells (one-double targeting) *in vivo*.

The results are similar whatever the absence or presence of 10% fetal bovine serum in cell culture medium, indicating that nonspecific interactions should not occur between the NLC and serum proteins. The dense polyethylene glycol coating of the nanoparticles seems to be efficient in preventing protein binding.

3.7. *In Vivo* Therapeutic Experiment. Antitumor activity was evaluated at a dose of 20 mg/kg administered by intravenous route. The antitumor effect (in terms of tumor growth) was shown in Figure 9. Obvious tumor regression was observed in mice treated with Duopafei, nNLC and tNLC, while no antitumor effect was observed in the group of N.S, blank nNLC and blank tNLC. It was found that the tumor volumes treated with tNLC were smaller than those treated with nNLC ($P < 0.05$) and the antitumor effects of the NLC (nNLC and tNLC) group were much stronger than that of the Duopafei group ($P < 0.01$) at the same dose. At the end of the test, tumor volume in mice treated with tNLC was 0.20 ± 0.35 cm^3, which was significantly smaller than the value of 1.23 ± 0.90 cm^3 for the Duopafei group ($P < 0.01$).

These results suggested that tNLC, as a target drug delivery system, could specifically target chemotherapeutic agents to tumors which overexpress VEGFR-2 via anti-VEGFR-2 antibody *in vivo*. We speculated that the high antitumor activity of tNLC was achieved by the following mechanisms. First, tNLC and nNLC both could accumulate in tumor tissue, ultimately reaching high levels in tumor due to the enhanced permeability and retention effect.[33] Then, tNLC bind to and internalize in tumor

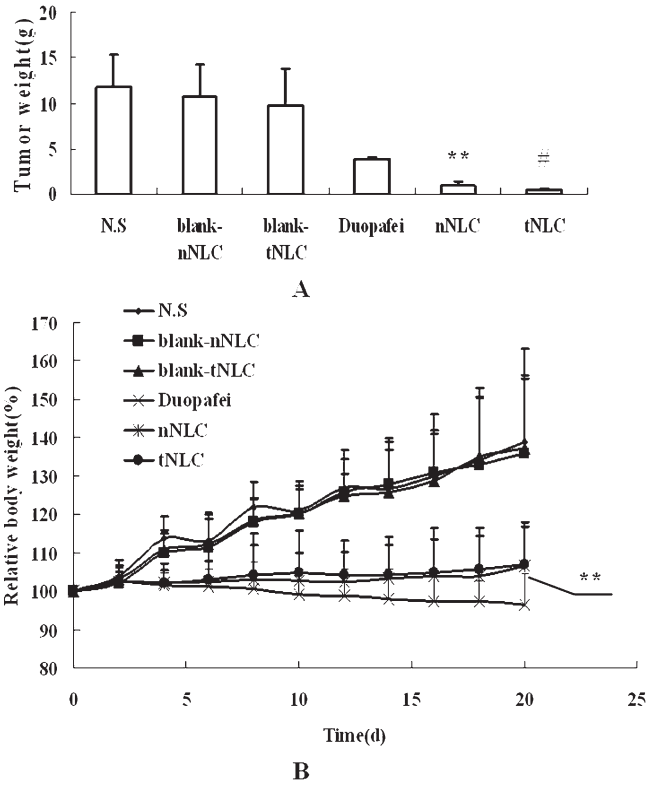

Figure 10. Tumor weight (A) and variation of body weight (B) by intravenous administration in B16 tumor-bearing mice (n = 6). Note: $^{**}P < 0.01$ versus Duopafei; $^{\#}P < 0.05$ versus nNLC.

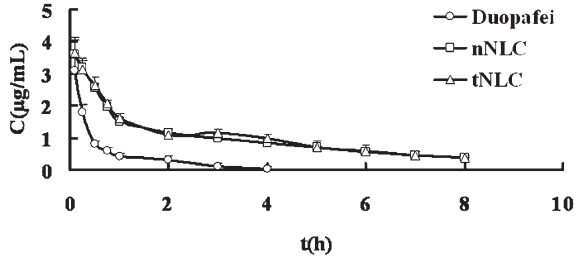

Figure 11. Mean plasma concentration of DTX after intravenous administration of Duopafei, nNLC and tNLC. Data represent mean ± SD (n = 5).

cells and tumor neovasculatures via ligand−receptor interactions, resulting in a potent antitumor activity. In contrast, nNLC remain in the interstitial space and are subject to decomposition, degradation or phagocytosis, with resulting release of drug. Detailed studies on mechanism of ligand−receptor interactions are under our further study.

Figure 10B shows the body weight variations of mice during the experimental period; obvious body weight loss of the mice treated with Duopafei was observed compared with the other two NLC groups ($P < 0.01$). The analysis of body weight variations could be used to define the adverse effects of the different therapy regiments. These results led to a conclusion that nNLC and tNLC generated less toxicity to mice than Duopafei when administered intravenously under the present experimental conditions, which will facilitate its future clinical application. Moreover, the mice receiving Duopafei were observed in a weak state, whereas no obvious alteration was observed in the NLC-treated animals.

Table 2. The Pharmacokinetic Parameters of DTX Formulations after Intravenous Administration (n = 5)

	formulations		
pharmacokinetic parameters	Duopafei	nNLC	tNLC
$t_{1/2\alpha}$ (h)	0.16 ± 0.05	0.32 ± 0.05^{**a}	0.30 ± 0.04*
$t_{1/2\beta}$ (h)	1.26 ± 0.16	3.92 ± 0.26**	3.57 ± 0.24**
$AUC_{0-\infty}$ (mg L^{-1} h)	2.58 ± 0.23	10.75 ± 0.43**	10.86 ± 0.54**
MRT (h)	0.91 ± 0.14	4.73 ± 0.56**	4.40 ± 0.35**
CL (L h^{-1} kg^{-1})	7.75 ± 0.73	1.86 ± 0.24**	1.84 ± 0.25**
T_{max} (h)	0.083	0.083	0.083
C_{max} (μgmL^{-1})	3.10 ± 0.44	3.60 ± 0.43	3.66 ± 0.45

^{a} $^*P < 0.05$, $^{**}P < 0.01$ vs Duopafei.

Overall, these findings indicate that tNLC showed a higher efficacy in a murine malignant melanoma model when compared with nNLC. Compared with Duopafei, nNLC and tNLC showed higher efficacy and lower side effects in a murine malignant melanoma model.

3.8. Pharmacokinetic Studies and Biodistribution of NLC. The concentration in plasma versus time profile of DTX after intravenous administration of the three formulations in mice is shown in Figure 11. After injection of nNLC and tNLC, the DTX in serum was still measurable after 8 h, while was not detectable even after 4 h for the Duopafei group. There was no statistical significance of DTX serum concentration between nNLC and tNLC. The pharmacokinetic parameters after intravenous administration of the three DTX formulations are summarized in Table 2.

The analysis of the results of the pharmacokinetic study data by the DAS (2.0) program indicates that all formulations fitted to the two-compartment model following intravenous administration. The $AUC_{0-\infty}$ following intravenous administration of tNLC and nNLC was significantly higher than that of Duopafei ($P < 0.01$). The relative bioavailability of tNLC and nNLC to Duopafei was 417% and 421%, respectively. The nNLC and tNLC significantly enhanced the half-life of DTX. Compared with the Duopafei, MRT and $t_{1/2\beta}$ of nNLC increased by about 4.20 and 2.11 times, respectively, while CL decreased by 3.17 times. Compared with the Duopafei, MRT and $t_{1/2\beta}$ of tNLC increased by about 3.44 and 1.83 times, respectively, while CL decreased by 3.21 times.

The tissue DTX concentrations versus time after intravenous administration of Duopafei, nNLC and tNLC are shown in Figure 12 and Table 3. As shown in Figure 12, the concentration of DTX was high in the heart and kidney after intravenous administration of Duopafei, which could cause side effects. Both of the NLC formulations decreased the DTX concentration in the heart and kindey, which would then be expected to reduce the side effects of the drug. The accumulation of nNLC and tNLC in liver, spleen and lung was higher than that of Duopafei.

Furthermore, tNLC resulted in substantial accumulation of DTX in tumor, and tumor accumulation in the tNLC group was significantly greater than in nNLC groups and far superior to the Duopafei, as shown in Table 3 and Figure 13. The overall targeting efficiency (T_e) of tNLC in tumor was improved from 4.04% (Duopafei) to 6.41% (1.59 times), the relative targeting efficiency (r_e) and the maximum concentrations (C_e) in tumor were 2.63 and 1.35 respectively; T_e of nNLC in tumor was improved from 4.04% (Duopafei) to 4.54% (1.12 times), and

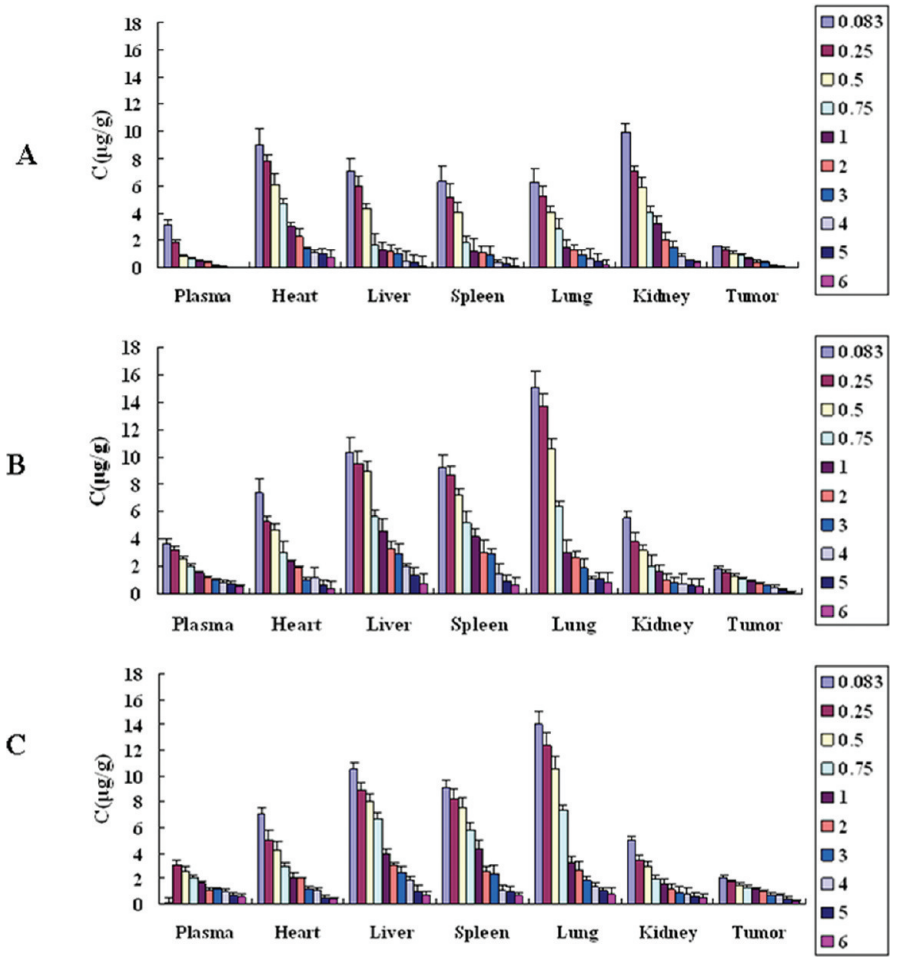

Figure 12. Mean tissue concentration of DTX after intravenous administration of Duopafei (A), nNLC (B) and tNLC (C). Data represent mean ± SD (n = 5).

Table 3. Targeting Disposition of DTX after Intravenous Administration of Duopafei, nNLC and tNLC to Mice (n = 5)

	Duopafei	nNLC			tNLC		
tissues	T_e (%)	T_e (%)	r_e	C_e	T_e (%)	r_e	C_e
heart	27.62	11.06	0.68	0.81	11.29	0.68	0.78
liver	13.40	22.64	2.88	1.47	20.85	2.58	1.50
spleen	12.19	19.28	2.70	1.47	18.58	2.53	1.43
lung	15.63	21.03	2.29	2.40	21.81	2.32	2.23
kidney	22.76	10.80	0.81	0.55	10.01	0.73	0.50
tumor	4.04	4.54	1.92	1.16	6.41	2.63	1.35
plasma	4.36	10.65	4.17	1.16	11.05	4.21	1.18

r_e and C_e in tumor were 1.92 and 1.16, respectively. The relative tumor accumulation of nNLC and tNLC to Duopafei at 6 h after intravenous administration was 294% and 533%, respectively.

The mechanisms of targeting nanocarriers to a particular disease are generally categorized as either active or passive targeting strategies. Active targeting involves the use of disease-specific targeting ligands such as antibodies (antigen targeting), lectins (carbohydrate targeting), and peptides (receptor targeting). Active targeting has the ability to improve the therapeutic index

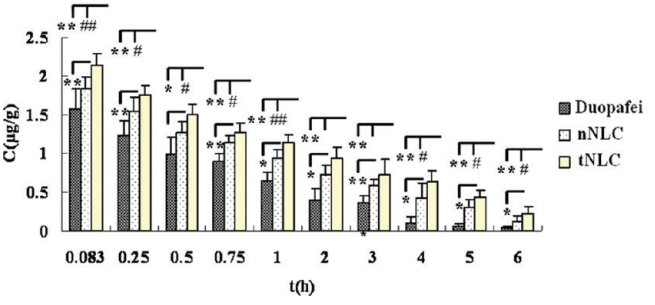

Figure 13. Distribution of DTX in tumor tissues after intravenous administration of Duopafei, nNLC and tNLC to mice at 0.083, 0.25, 0.5, 0.75, 1, 2, 3, 4, 5, and 6 h (n = 5). Note: $^{*}P < 0.05$, $^{**}P < 0.01$ versus Duopafei; $^{\#}P < 0.05$, $^{\#\#}P < 0.01$ versus nNLC.

of biologically active agents by increasing target-site accumulation and by improving the pharmacokinetics of the system and drugs. In this study both the nontargeted and the targeted NLC provided biodistribution and pharmacokinetic advantages relative to Duopafei. The quantitative and qualitative biodistribution profiles of both nanoparticle formulations were almost identical. These illustrated that the minute difference between the two formulations (approximately 3% surface modification with the

anti-VEGFR2 antibody) was not enough to alter the biodistribution of NLC, and the size of NLC was the crucial factor for biodistribution of nontargeted and the targeted NLC.[34] This antibody modification was, however, enough to alter the pharmacokinetic profile of the NLC. The tumor accumulation for the tNLC group was significantly greater than for nNLC groups and far superior to the Duopafei.

In cancer therapy, to obtain active targeting to tumors, recently, some considerations have been given to the host endothelial cell of tumor neovasculature.[35−37] For example, developing and testing a drug delivery system should be analyzed for its ability to target to the endothelial cells of tumor vessels, and not just the tumor cells. As described previously,[7,8] VEGFRs have been found to be overexpressed, in comparison to normal tissues, in breast, melanoma, gastric, and non-small-cell lung cancer and on tumor neovasculature in situ. In this work, we have achieved "double-targeting" antitumor therapy through one drug delivery system, both of which have attracted considerable attention: the targeting of antitumor therapeutics to tumor cells via ligands against receptors which are overexpressed on the surface of many types of cancer cells and are not overexpressed detectably in normal organs, and the targeting of antitumor therapeutics to the tumor vasculature via ligands directed selectively against tumor vasculature endothelial cells. In addition, passive targeting takes advantage of the size of nanoparticles and the unique properties of tumor vasculature, such as the EPR effect.[37] Angiogenic blood vessels in tumor tissues, unlike those in normal tissues (nearly 100 nm), have gaps as large as 400 to 800 nm between adjacent endothelial cells, thereby, the particle size of tNLC is too big to penetrate into normal tissues but still small enough to extravasate through the leaky capillaries in the tumor tissue with minimal uptake by normal tissues.

Taken together, we demonstrated that the VEGFR-mediated drug delivery system has several advantages that are necessary in cancer therapy: (1) enhanced specific cellular uptake and penetration in tumor cells; (2) maximal accumulation and penetration into tumor site via anti-VEGFR-2 antibody which could bind specifically to VEGFR2 on tumors; (3) "one-double targeting" tumor therapies (tumor and vascular targeting) via solo drug delivery system; (4) less toxicity to normal organs and tissues as compared with Duopafei. This progress is vital to the application of target therapy strategies.

4. CONCLUSIONS

Here we report for the first time that Flk (A-3) modified DTX loaded NLC demonstrated superior antitumor efficacy against malignant melanoma both *in vitro* and *in vivo*. In summary, tNLC, as a drug delivery system, achieved favorable tumor and vascular-targeted drug delivery and antitumor effects are due to specific binding and internalization of tumor cells and tumor microvasculature via anti-VEGFR-2 antibody. Although further investigation on the precise transfer mechanism of tNLC is required, the findings of our study represent an important step in advancing the one-double targeting strategy to treat tumors that overexpress VEGFR-2.

AUTHOR INFORMATION

Corresponding Author

*Shandong University, School of Pharmaceutical Sciences, Institute of Pharmaceutics, 44 Wenhua Xi Road, Ji'nan 250012, China. Tel: +86 531 88382015. Fax: +86 531 88382548. E-mail: zhangnancy9@sdu.edu.cn.

ACKNOWLEDGMENT

The Project was supported by Program for New Century Excellent Talents in University (NCET-08-0334).

REFERENCES

(1) Cheong, I.; Huang, X.; Bettegowda, C.; Diaz, L. A., Jr.; Kinzler, K. W.; Zhou, S. B.; Vogelstein, B. A bacterial protein enhances the release and efficacy of liposomal cancer drugs. *Science* **2006**, *314* (5803), 1308–11.

(2) Lotfi-Jam, K.; Carey, M.; Jefford, M.; Schofield, P.; Charleson, C.; Aranda, S. Nonpharmacologic strategies for managing common chemotherapy adverse effects: a systematic review. *J. Clin. Oncol.* **2008**, *26* (34), 5618–29.

(3) Dharap, S. S.; Wang, Y.; Chandna, P.; Khandare, J. J.; Qiu, B.; Gunaseelan, S.; Sinko, P. J.; Stein, S.; Farmanfarmaian, A.; Minko, T. Tumor-specific targeting of an anticancer drug delivery system by LHRH peptide. *Proc. Natl. Acad. Sci. U.S.A.* **2005**, *102* (36), 12,962–7.

(4) Moghimi, S. M.; Hunter, A. C.; Murray, J. C. Nanomedicine: current status and future prospects. *FASEB J.* **2005**, *19* (3), 311–30.

(5) Dings, R. P.; Van Laar, E. S.; Webber, J.; Zhang, Y.; Griffin, R J.; Waters, S. J.; MacDonald, J. R.; Mayo, K. H. Ovarian tumor growth regression using a combination of vascular targeting agents anginex or topomimetic 0118 and the chemotherapeutic irofulven. *Cancer Lett.* **2008**, *265* (2), 270–80.

(6) Tyler, M. A.; Ulasov, I. V.; Borovjagin, A.; Sonabend, A. M.; Khramtsov, A.; Han, Y.; Dent, P.; Fisher, P. B.; Curiel, D. T.; Lesniak, M. S. Enhanced transduction of malignant glioma with a double targeted Ad5/3-RGD fibermodified adenovirus. *Mol. Cancer Ther.* **2006**, *5* (9), 2408–16.

(7) Tol, J.; Punt, C. J. Monoclonal Antibodies in the Treatment of Metastatic Colorectal Cancer: A Review. *Clin. Ther.* **2010**, *32* (3), 437–53.

(8) Veenendaal, L. M.; Jin, H.; Ran, S.; Cheung, L.; Navone, N.; Marks, J. W.; Waltenberger, J.; Thorpe, P.; Rosenblum, M. G. In vitro and in vivo studies of a VEGF121/rGelonin chimeric fusion toxin targeting the neovasculature of solid tumors. *Proc. Natl. Acad. Sci. U.S.A.* **2002**, *99* (12), 7866–71.

(9) Roth, P.; Hammer, C.; Piguet, A. C.; Ledermann, M.; Dufour, J. F.; Waelti, E. Effects on hepatocellular carcinoma of doxorubicin-loaded immunoliposomes designed to target the VEGFR-2. *J. Drug Targeting* **2007**, *15* (9), 623–31.

(10) Thirumamagal, B. T.; Zhao, X. B.; Bandyopadhyaya, A. K.; Naranyanasamy, S.; Johnsamuel, J.; Tiwari, R.; Golightly, D. W.; Patel, V.; Jehning, B. T.; Backer, M. V.; Barth, R. F.; Lee, R. J.; Backer, J. M.; Tjarks, W. Receptor-targeted liposomal delivery of boron-containing cholesterol mimics for boron neutron capture therapy (BNCT). *Bioconjugate Chem.* **2006**, *17* (5), 1141–50.

(11) Rubio Demirovic, A.; Marty, C.; Console, S.; Zeisberger, S. M.; Ruch, C.; Jaussi, R.; Schwendener, R. A.; Ballmer-Hofer, K Targeting human cancer cells with VEGF receptor-2-directed liposomes. *Oncol. Rep.* **2005**, *13* (2), 319–24.

(12) Kunkel, P.; Ulbricht, U.; Bohlen, P.; Brockmann, M. A.; Fillbrandt, R.; Stavrou, D.; Westphal, M.; Lamszus, K. Inhibition of glioma angiogenesis and growth in vivo by systemic treatment with a monoclonal antibody against vascular endothelial growth factor receptor-2. *Cancer Res.* **2001**, *61* (18), 6624–8.

(13) Spratlin, J. L.; Cohen, R. B.; Eadens, M.; Gore, L.; Camidge, D. R.; Diab, S.; Leong, S.; O'Bryant, C.; Chow, L. Q.; Serkova, N. J.; Meropol, N. J.; Lewis, N. L.; Chiorean, E. G.; Fox, F.; Youssoufian, H.; Rowinsky, E. K.; Eckhardt, S. G. Phase I pharmacologic and biologic study of ramucirumab (IMC-1121B), a fully human immunoglobulin G1 monoclonal antibody targeting the vascular endothelial growth factor receptor-2. *J. Clin. Oncol.* **2010**, *28* (5), 780–7.

(14) Tanno, S.; Ohsaki, Y.; Nakanishi, K.; Toyoshima, E.; Kikuchi, K. Human small cell lung cancer cells express functional VEGF receptors, VEGFR-2 and VEGFR-3. *Lung Cancer* **2004**, *46* (1), 11–9.

(15) Müller, R. H.; Radtke, M.; Wissing, S. A. Solid lipid nanoparticles (SLN) and nanostructured lipid carriers (NLC) in cosmetic and dermatological preparations. *Adv. Drug Delivery Rev.* **2002**, *54* (Suppl. 1), S131–55.

(16) Souto, E. B.; Müller, R. H. Lipid nanoparticles: effect on bioavailability and pharmacokinetic changes. *Handb. Exp. Pharmacol.* **2010**, *197*, 115–41.

(17) Saloustros, E.; Georgoulias, V. Docetaxel in the treatment of advanced non-small-cell lung cancer. *Expert Rev. Anticancer Ther.* **2008**, *8* (8), 1207–22.

(18) Saloustros, E.; Mavroudis, D.; Georgoulias, V. Paclitaxel and docetaxel in the treatment of breast cancer. *Expert Opin. Pharmacother.* **2008**, *9* (15), 2603–16.

(19) Haass, N. K.; Sproesser, K.; Nguyen, T. K.; Contractor, R.; Medina, C. A.; Nathanson, K. L.; Herlyn, M.; Smalley, K. S. The mitogen-activated protein/ extracellular signal-regulated kinase kinase inhibitor AZD6244 (ARRY-142886) induces growth arrest in melanoma cells and tumor regression when combined with docetaxel. *Clin. Cancer Res.* **2008**, *14* (1), 230–9.

(20) Nakatsu, M. N.; Sainson, R. C.; Aoto, J. N.; Taylor, K. L; Aitkenhead, M.; Pérez-del-Pulgar, S.; Carpenter, P. M.; Hughes, C. C. Angiogenic sprouting and capillary lumen formation modeled by human umbilical vein endothelial cells (HUVEC) in fibrin gels: the role of fibroblasts and Angiopoietin-1. *Microvasc. Res.* **2003**, *66* (2), 102–12.

(21) Sun, T.; Sun, B. C.; Ni, C. S.; Zhao, X. L.; Wang, X. H.; Qie, S.; Zhang, D. F.; Gu, Q.; Qi, H.; Zhao, N. Pilot study on the interaction between B16 melanoma cell-line and bone-marrow derived mesenchymal stem cells. *Cancer Lett.* **2008**, *263* (1), 35–43.

(22) Xu, X.; Wang, S.; Chen, W.; Chen, G. Effects of taohong siwu decoction II in the chick chorioallantoic membrane (CAM) assay and on B16 melanoma in mice and endothelial cells ECV304 proliferation. *J. Tradit. Chin. Med.* **2006**, *26* (1), 63–7.

(23) Curnis, F.; Sacchi, A.; Gasparri, A.; Longhi, R.; Bachi, A.; Doglioni, C.; Bordignon, C.; Traversari, C.; Rizzardi, G. P.; Corti, A. Isoaspartate-glycine-arginine: a new tumor vasculature-targeting motif. *Cancer Res.* **2008**, *68* (17), 7073–82.

(24) Yanasarn, N.; Sloat, B. R.; Cui, Z. Nanoparticles engineered from lecithin-in-water emulsions as a potential delivery system for docetaxel. *Int. J. Pharm.* **2009**, *379* (1), 174–80.

(25) Hureaux, J.; Lagarce, F.; Gagnadoux, F.; Vecellio, L.; Clavreul, A.; Roger, E.; Kempf, M.; Racineux, J. L.; Diot, P.; Benoit, J. P.; Urban, T. Lipid nanocapsules: Ready-to-use nanovectors for the aerosol delivery of paclitaxel. *Eur. J. Pharm. Biopharm.* **2009**, *73* (2), 239–46.

(26) Zhang, J.; Qian, Z.; Gu, Y. In vivo anti-tumor efficacy of docetaxel-loaded thermally responsive nanohydrogel. *Nanotechnology* **2009**, *20* (32), 325102.

(27) Pastorino, F.; Brignole, C.; Di Paolo, D.; Nico, B.; Pezzolo, A.; Marimpietri, D.; Pagnan, G.; Piccardi, F.; Cilli, M.; Longhi, R.; Ribatti, D.; Corti, A.; Allen, T. M.; Ponzoni, M. Targeting liposomal chemotherapy via both tumor cell-specific and tumor vasculature-specific ligands potentiates therapeutic efficacy. *Cancer Res.* **2006**, *66* (20), 10073–82.

(28) Oba, M.; Fukushima, S.; Kanayama, N.; Aoyagi, K.; Nishiyama, N.; Koyama, H.; Kataoka, K. Cyclic RGD peptide-conjugated polyplex micelles as a targetable gene delivery system directed to cells possessing alphavbeta3 and alphavbeta5 integrins. *Bioconjugate Chem.* **2007**, *18* (5), 1415–23.

(29) Kolonin, M. G.; Sun, J.; Do, K. A.; Vidal, C. I.; Ji, Y.; Baggerly, K. A.; Pasqualini, R.; Arap, W. Synchronous selection of homing peptides for multiple tissues by in vivo phage display. *FASEB J.* **2006**, *20* (7), 979–81.

(30) Zheng, D.; Li, X.; Xu, H.; Lu, X.; Hu, Y.; Fan, W. Study on docetaxel-loaded nanoparticles with high antitumor efficacy against malignant melanoma. *Acta Biochim. Biophys. Sin. (Shanghai)* **2009**, *41* (7), 578–87.

(31) Le Garrec, D.; Gori, S.; Luo, L.; Lessard, D.; Smith, D. C.; Yessine, M. A.; Ranger, M.; Leroux, J. C. Poly(N-vinylpyrrolidone)-block-poly(D,L-lactide) as a new polymeric solubilizer for hydrophobic anticancer drugs: in vitro and in vivo evaluation. *J. Controlled Release* **2004**, *99* (1), 83–101.

(32) Doktorovova, S.; Souto, E. B. Nanostructured lipid carrier-based hydrogel formulations for drug delivery: a comprehensive review. *Expert Opin. Drug Delivery* **2009**, *6* (2), 165–76.

(33) Wang, X.; Yang, L.; Chen, Z. G.; Shin, D. M. Application of nanotechnology in cancer therapy and imaging. *Ca—Cancer J. Clin.* **2008**, *58* (2), 97–110.

(34) Milane, L.; Duan, Z. F.; Amiji, M. Pharmacokinetics and biodistribution of lonidamine/paclitaxel loaded, EGFR-targeted nanoparticles in an orthotopic animal model of multi-drug resistant breast cancer. *Nanomedicine* **2011**, *7* (4), 435–44.

(35) Kerbel, R. S. Tumor angiogenesis: past, present and the near future. *Carcinogenesis* **2000**, *21* (3), 505–15.

(36) Shchors, K.; Evan, G. Tumor angiogenesis: cause or consequence of cancer? *Cancer Res.* **2007**, *67* (15), 7059–61.

(37) Murphy, E. A.; Majeti, B. K.; Barnes, L. A.; Makale, M.; Weis, S. M.; Lutu-fuga, K.; Wrasidlo, W.; Cheresh, D. A. Nanoparticle-mediated drug delivery to tumor vasculature suppresses metastasis. *Proc. Natl. Acad. Sci. U.S.A.* **2008**, *105* (27), 9343–8.